Ephrin-A3 promotes and maintains slow muscle fiber identity during postnatal development and reinnervation

Danny A. Stark,[1,2] Nathan J. Coffey,[1] Hannah R. Pancoast,[1] Laura L. Arnold,[1,2] J. Peyton D. Walker,[2] Joanne Vallée,[3] Richard Robitaille,[3,4] Michael L. Garcia,[1,2] and DDW Cornelison[1,2]

[1]Division of Biological Sciences and [2]Christopher S. Bond Life Sciences Center, University of Missouri, Columbia, MO 65211
[3]Département de Neurosciences and [4]Groupe de Recherche sur le Système Nerveux Central, Université de Montréal, Montréal, Québec H3C 3J7, Canada

Each adult mammalian skeletal muscle has a unique complement of fast and slow myofibers, reflecting patterns established during development and reinforced via their innervation by fast and slow motor neurons. Existing data support a model of postnatal "matching" whereby predetermined myofiber type identity promotes pruning of inappropriate motor axons, but no molecular mechanism has yet been identified. We present evidence that fiber type–specific repulsive interactions inhibit innervation of slow myofibers by fast motor axons during both postnatal maturation of the neuromuscular junction and myofiber reinnervation after injury. The repulsive guidance ligand ephrin-A3 is expressed only on slow myofibers, whereas its candidate receptor, EphA8, localizes exclusively to fast motor endplates. Adult mice lacking ephrin-A3 have dramatically fewer slow myofibers in fast and mixed muscles, and misexpression of ephrin-A3 on fast myofibers followed by denervation/reinnervation promotes their respecification to a slow phenotype. We therefore conclude that Eph/ephrin interactions guide the fiber type specificity of neuromuscular interactions during development and adult life.

Introduction

Vertebrate skeletal muscle development, which has been best studied in the context of the limb musculature, is a stepwise, progressive process of specification, commitment, and differentiation. Progenitor cells originating in the somite emigrate laterally into the nascent limb buds beginning at embryonic day (E) 10.5 in the mouse, followed by myogenic specification in response to local environmental cues (Kardon et al., 2002). Embryonic myoblasts condense into premuscle masses, terminally differentiate into myocytes, and form primary myofibers that prepattern the alignment and morphology of the mature muscle (Emerson and Hauschka, 2004). From E14.5 to E20.5, a second population of myoblasts (fetal myoblasts) expands in the muscle primordia and differentiates, fusing with each other into larger, multinucleated secondary myofibers aligned with primary myofibers. Also during late prenatal muscle development, motor neurons extend axons from the spinal cord into the developing musculature to synapse with the newly formed myofibers; processes from up to 10 different axons may be located at the motor endplate of a single myofiber at birth. During the first 1–3 wk after birth, each myofiber loses its synaptic connections with all but one of the motor axons assembled at the motor endplate and the remaining axon overtakes the surface of the motor endplate, forming the mature neuromuscular junction (NMJ) that transmits electrical impulses to the myofiber (Sanes and Lichtman, 1999).

Expression of different myosin heavy chains (MyHCs) confers distinct physiological and functional properties on different myofibers; thus, fiber type specification is a critical component of muscle morphogenesis. Mature myofibers in the adult generally express either slow MyHC (MyHC-I) or one of three fast MyHCs (MyHC-IIa, MyHC-IId/x, or MyHC-IIb). Muscle fiber type and MyHC expression remains plastic until myofibers are monoinnervated and incorporated into a motor unit during postnatal development (Sanes and Lichtman, 1999). Reflecting the function of the myofibers they innervate, motor neurons are classified as slow, fast-resistant, and fast-fatigable based on their electrical firing rate, their threshold of activation, and refractory time (Garnett et al., 1979; Hamm et al., 1988); at steady state in mature muscle, it is the frequency of electrical stimulation characteristic to each neuron type that specifies the fiber type and MyHC gene expression of the myofibers it innervates

Correspondence to DDW Cornelison: cornelisond@missouri.edu

D.A. Stark's present address is Vision Research Center, Dept. of Ophthalmology, School of Medicine, University of Missouri–Kansas City, Kansas City, MO 64108.

Abbreviations used in this paper: EDL, extensor digitorum longus; MyHC, myosin heavy chain; NMJ, neuromuscular junction; TA, tibialis anterior.

The Rockefeller University Press $30.00
J. Cell Biol. Vol. 211 No. 5 1077–1091
www.jcb.org/cgi/doi/10.1083/jcb.201502036

(Kanning et al., 2010). The extent to which the neuronal influence dominates is shown by the nearly complete switching of MyHC expression that results when an inappropriate neuronal connection is provided experimentally: a normally fast muscle will switch its phenotype to slow when it is cross-reinnervated in early postnatal life by a nerve that would normally innervate a slow muscle (Buller et al., 1960). The same effect can be produced by direct electrical stimulation of denervated muscles at the frequencies characteristic of either slow or fast motor axons (Pette and Vrbová, 1985), although the efficiency with which such conversion can occur is dependent on the original fiber type composition of the muscle. This phenomenon is also reflected in the observation that all mature myofibers innervated by the same motor neuron (i.e., a single motor unit) express the same MyHC (Nemeth et al., 1981).

Mechanisms that have been proposed to account for the matching of neuron to myofiber include guidance (motor axons are directed to specific myofibers by cues not directly associated with the myofibers themselves); conversion (previously equivalent myofibers are converted to a phenotype consistent with their innervation); and recognition (motor axons and myofibers express cell surface markers that confer mutual recognition). Among these, the preponderance of evidence supports the idea that recognition between neurons and myofibers is key to postnatal patterns of innervation (Sanes and Lichtman, 1999). Intriguingly, another aspect of muscle identity that shows specificity of innervation is position on the rostrocaudal axis, for which both muscle and nerves possess a heritable identity (Donoghue et al., 1992a) that promotes interactions between cells originating at the same level. This specificity appears to be a result of differential expression of specific ephrins (a family of cell surface contact-mediated repulsive ligands) on myofibers that prevents interactions with neurons from inappropriate axial levels (Donoghue et al., 1996; Feng et al., 2000; Chadaram et al., 2007).

Ephrin ligands and their Eph receptors have pleiotropic roles in many developmental processes, such as neural crest cell migration and axon guidance (Krull et al., 1997; Wang and Anderson, 1997). In muscle development, ephrin signaling has been shown to be important for myoblast migration into the limb (Swartz et al., 2001), early motor axon guidance (Iwamasa et al., 1999), and topographical organization of innervation across muscle fibers (Feng et al., 2000). Our previous work identified the potential for Eph/ephrin-based repulsive interactions between mature myofibers in the adult and the stem cells of skeletal muscle (satellite cells) as well as effects on differentiated muscle patterning (Stark et al., 2011), but Eph/ephrin expression patterns also differ between embryonic and adult muscle and between homeostasis and regeneration (Lai et al., 2001; Stark et al., 2011), thus complicating the search for a conserved role in muscle patterning.

In this study, we have expanded on our prior results to show that ephrin-A3 is expressed exclusively by slow myofibers in the adult. Using ephrin-A3 loss-of-function and gain-of-function approaches, we have generated a model in which muscle/nerve interactions via ephrin-A3 and EphA8 promote slow myofiber specification, maintenance, and repair by discouraging innervation by motor neurons that would impose a fast phenotype. These data support a model in which preferential elimination of synapses with fast motor axons during postnatal axon pruning determines the final composition of the mature NMJ and imposes adult myofiber type.

Results

Ephrin-A3 is expressed on all and only MyHC-I^{+ve} (slow) myofibers

In our prior immunohistochemical screen of Eph and ephrin expression in adult muscle, we noted that of the eight ephrin ligands, only ephrin-A3 showed differential expression among individual myofibers (Stark et al., 2011). To further characterize the myofibers expressing ephrin-A3, we correlated ephrin-A3 immunopositivity with sarcomeric MyHC expression in the uninjured gastrocnemius, plantaris, soleus, tibialis anterior (TA), and extensor digitorum longus (EDL) muscles. We found that ephrin-A3 specifically marks all slow myofibers (Fig. 1, A and B) in each muscle examined; in contrast, fast myofibers expressing MyHC-IIa (Fig. 1, C and D) or MyHC-IIb (Fig. 1, E and F) never express ephrin-A3. Expression of MyHC-IIx, for which there are no commercial antibodies, was presumed in myofibers expressing none of the other three isoforms (Waddell et al., 2010; Chakkalakal et al., 2012), and these unlabeled myofibers also never expressed ephrin-A3. We scored and averaged the number of slow myofibers in the TA, EDL, and soleus muscles ($n = 3$ for each muscle) and found that they contain 0.26%, 4%, and 42% MyHC-I^{+ve} myofibers, respectively (Fig. 1 G), consistent with the existing literature (Augusto et al., 2004). Individual muscles are known to maintain their unique fiber type distribution in a healthy adult even after regeneration (Wigmore and Evans, 2002), so we hypothesized that ephrin-A3 could be a mediator of muscle fiber type specification and/or maintenance.

Deletion of ephrin-A3 leads to postnatal loss of slow myofibers

To test for a role in slow myofiber specification, we repeated the fiber type quantitation in homozygous ephrin-A3$^{-/-}$ adult mice (Carmona et al., 2009). We noted a striking decrease in slow myofibers in all but one major hindlimb muscle examined:the TA, EDL, and gastrocnemius only have 14% of the wild-type number of slow myofibers, and the plantaris has 27% of the wild-type number (Fig. 2). However, the total number of myofibers in each muscle does not change significantly between genotypes (not depicted) and, consistent with published work (Sanes and Lichtman, 1999), also does not change postnatally. Expression of MyHC-II isoforms is not altered significantly (Fig. S1), and, interestingly, MyHC-I expression in muscle spindle fibers appears to be unaffected in all ephrin-A3$^{-/-}$ muscles examined (not depicted). In contrast to the loss of MyHC-I^{+ve} myofibers in all other distal hind limb muscles, the number of MyHC-I^{+ve} myofibers in the soleus of ephrin-A3$^{-/-}$ mice did not change significantly (Fig. 2, B and C). Other groups have previously noted that developmental MyHC expression (Harris et al., 1989), slow myofiber specification (Gunning and Hardeman, 1991), and regeneration (Dolenc et al., 1994) in the soleus appear to involve mechanisms distinct from those in place in other hindlimb muscles, and studies of the fasciculation of predetermined populations of motor neurons also suggest that comparatively more slow axons would be expected to project into the soleus than into other hindlimb muscles (Rafuse et al., 1996; Milner et al., 1998).

Because the loss of slow myofibers in the adult ephrin-A3$^{-/-}$ mouse suggested a developmental effect, we analyzed expression of ephrin-A3 and MyHC-I in hindlimb muscles at developmental time points from E15.5 through postnatal day (P) 14. Although as expected, we detected robust expression

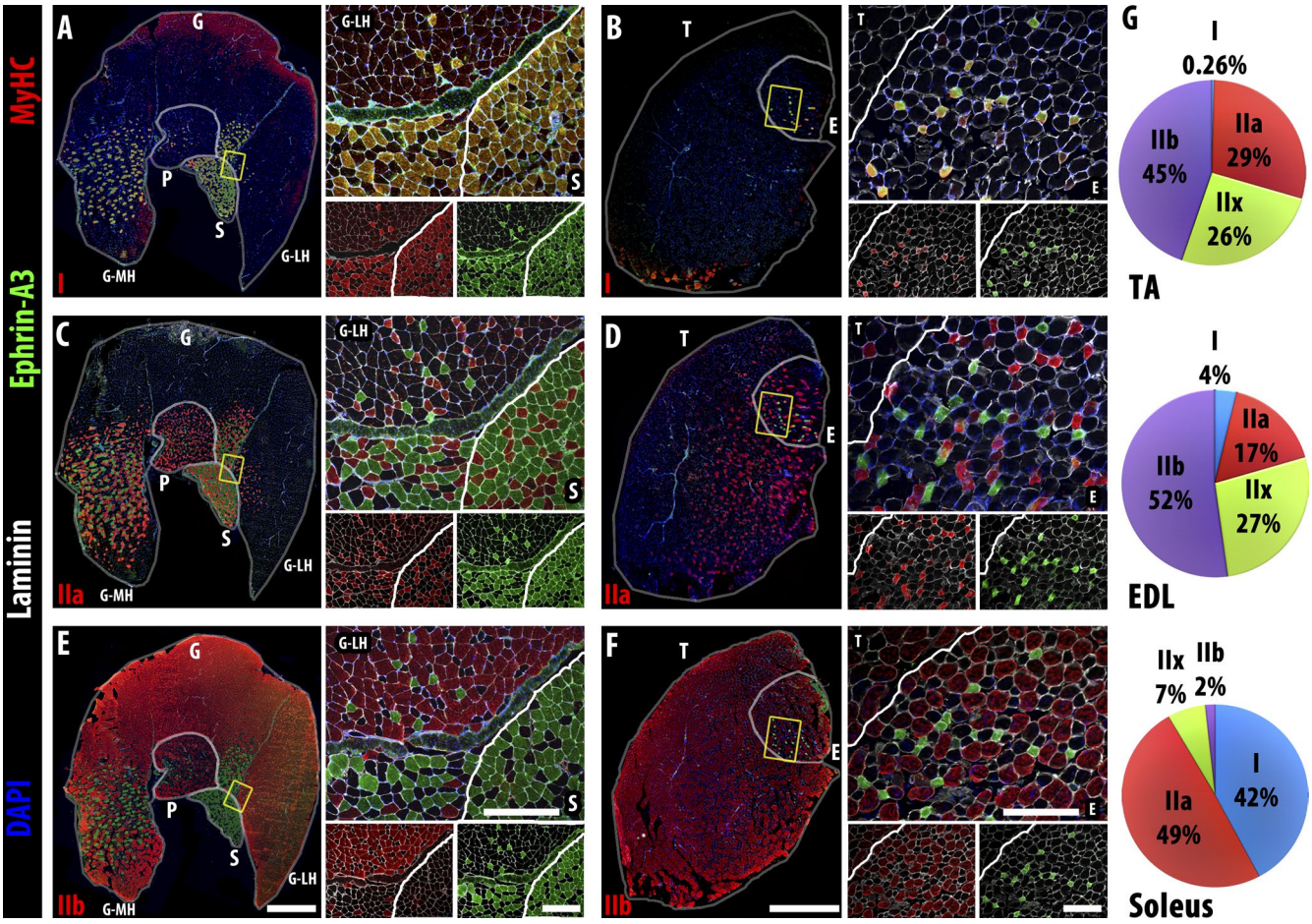

Figure 1. **Ephrin-A3 is expressed on all MyHC-I^{+ve} (slow) myofibers.** (A–F) Immunohistochemistry showing localization of ephrin-A3 (green) compared with two of three fast MyHCs (red: MyHC-I, top row; MyHC-IIa, middle row; and MyHC-IIb, bottom row), along with nuclei (DAPI, blue) and laminin (white) on transverse cryosections from uninjured gastrocnemius (G), plantaris (P), soleus (S), TA (T), and EDL (E) muscles. The yellow boxes in the left of each panel indicate the magnified regions on the top right, which are separated underneath to show expression of MyHC/laminin (left) and ephrin-A3/laminin (right). (A and B) All slow, MyHC-I^{+ve} myofibers in all muscles of the distal hindlimb express ephrin-A3. (C and D) No fast, MyHC-IIa^{+ve} myofibers in the distal hindlimb express ephrin-A3. (E and F) Ephrin-A3 is also never expressed by fast, MyHC-IIb^{+ve} myofibers. (G) Fiber type distribution of the TA, EDL, and soleus muscles (n = 3) in adult: each muscle has a unique and consistent ratio of the four myofiber types. Whole muscle montage gamma = 1.45. Bars: (montages) 1 mm; (insets) 300 µm. MH, gastrocnemius medial head; LH, lateral head.

of MyHC-I during embryonic muscle development (Fig. 3 A), significant ephrin-A3 expression is first noted later in development, after expression of MyHC-I (Fig. 3, B and C; and Fig. S2). Ephrin-A3 expression is rapidly up-regulated in MyHC-I^{+ve} myofibers from P1, and expression by all MyHC-I^{+ve} fibers is evident shortly thereafter.

When we quantified the number of MyHC-I–expressing myofibers in ephrin-A3$^{-/-}$ mice, we were somewhat surprised to find that it was indistinguishable from that of nontransgenic controls throughout embryonic and fetal development and continuing through the first 2 wk after birth (Fig. 4, A and B). However, we noted a significant decrease in the number of slow myofibers in ephrin-A3$^{-/-}$ mice between P14 and adulthood. Consistent with what has been reported previously (Whalen et al., 1984; Agbulut et al., 2003), during normal postnatal muscle development myofibers that had been initially expressing MyHC-I switch to a faster fiber type between birth and maturity. The degree of conversion differs between individual muscles: the TA and EDL both have ∼180 slow myofibers at birth and gradually lose ∼96% and 81%, respectively (Fig. 4 B), whereas the soleus maintains the same number of slow myofibers from birth to adulthood (Fig. S1 F). When we analyzed expression of MyHC-I and MyHC-IIa in serial sections of TA muscle from ephrin-A3$^{-/-}$ mice at P28 (Fig. 4 C), we saw that the majority of MyHC-I–expressing myofibers (Fig. 4 C, asterisks) were co-positive for MyHC-IIa and that the relative intensity of expression of MyHC-1 versus MyHC-IIa in these fibers reverses from P5 (MyHC-I^{high}) to P28 (MyHC-IIa^{high}; not depicted). Collectively, these data indicate that ephrin-A3 expression is a consequence rather than a cause of initial, cell-autonomous specification of slow myofibers, but then functions to preserve slow myofiber identity during the transition to non–cell-autonomous fiber type specification dictated by the motor neuron. Loss of this activity in ephrin-A3$^{-/-}$ muscles therefore permits innervation of previously slow myofibers by fast motor neurons, which is detectable at later stages by loss of MyHC-I expression.

Misexpression of ephrin-A3 in fast myofibers during reinnervation results in ectopic slow myofibers

We hypothesized that ephrin-A3 could promote slow myofiber specification and maintenance by preventing interactions with

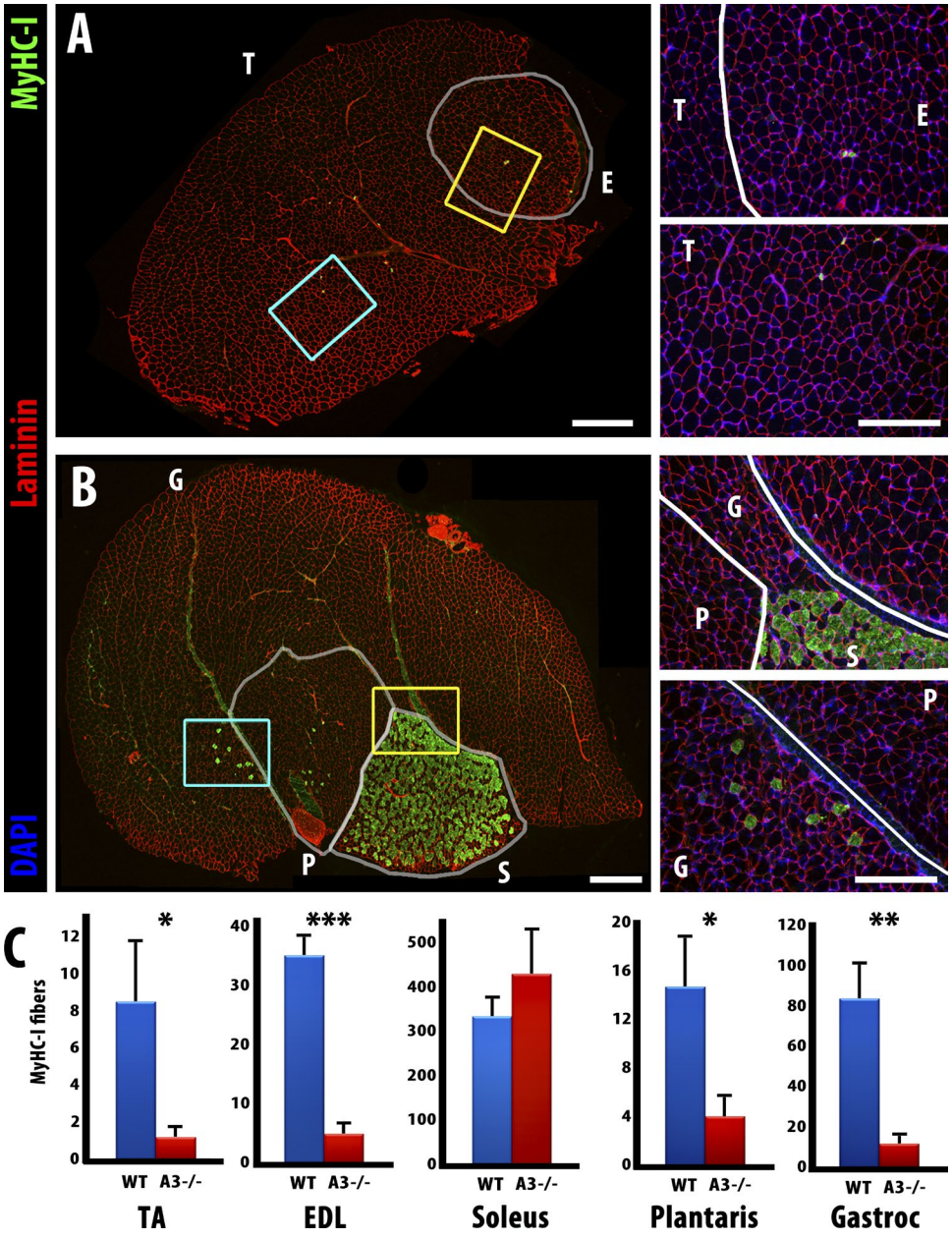

Figure 2. **Slow myofiber number is reduced in adult ephrin-A3$^{-/-}$ mice.** (A) Immunohistochemistry showing laminin (red) and MyHC-I (green) expression in transverse cryosections from uninjured TA (T) and EDL (E) muscles of an adult ephrin-A3$^{-/-}$ mouse. (B) Immunohistochemistry showing laminin (red) and MyHC-I (green) expression in transverse cryosections from uninjured gastrocnemius (G), plantaris (P), and soleus (S) muscles of an adult ephrin-A3$^{-/-}$ mouse. Inset areas are enlarged at right (yellow, top; cyan, bottom). (C) All but one muscle scored had significantly fewer MyHC-I^{+ve} myofibers in ephrin-A3$^{-/-}$ mice than age-matched wild type. P = 0.029 (TA); 0.0001 (EDL); 0.0035 (gastrocnemius); and 0.034 (plantaris). Error bars represent SEM. The change in MyHC-I^{+ve} myofibers in the soleus is not significant. *, P < 0.05; **, P < 0.005; ***, P < 0.0005. Bars: (montages) 500 µm; (insets) 300 µm. $n \geq 3$.

fast motor axons (and potentially other cell types) that would impose a fast phenotype. Thus, if loss of ephrin-A3 during development compromises the maintenance of slow myofibers, misexpression of ephrin-A3 on fast myofibers in the context of innervation or reinnervation could promote a shift to a slow fiber type. To test whether ephrin-A3 expression affects fiber type specification during muscle reinnervation, we used in vivo electroporation (Aihara and Miyazaki, 1998) to misexpress ephrin-A3 in fast myofibers of the TA (Fig. S3). In our hands, both GFP and ephrin-A3 expressed from the plasmid were extinguished by 4 wk after electroporation, although widespread and robust expression (variable between myofibers) is detectable within 3 d and sustained during the first 1–2 wk. We targeted the plasmid injection to the anterior region of the TA, which normally has no slow, ephrin-A3^{+ve} myofibers (Fig. 1 B). Electroporation with a control plasmid expressing GFP did not change the number of slow myofibers 4 wk after electroporation, even if the muscle was also challenged with denervation (Fig. 5 A, top.) Similarly, electroporation with ephrin-A3 plasmid alone (without inducing reinnervation) did not change the number of slow myofibers (Fig. 5 A, middle) and there were no ephrin-A3^{+ve} myofibers detected. However, when we electroporated with ephrin-A3 plasmid and then denervated the distal hindlimb by sciatic nerve crush 3 d later, we noted a dramatic increase in

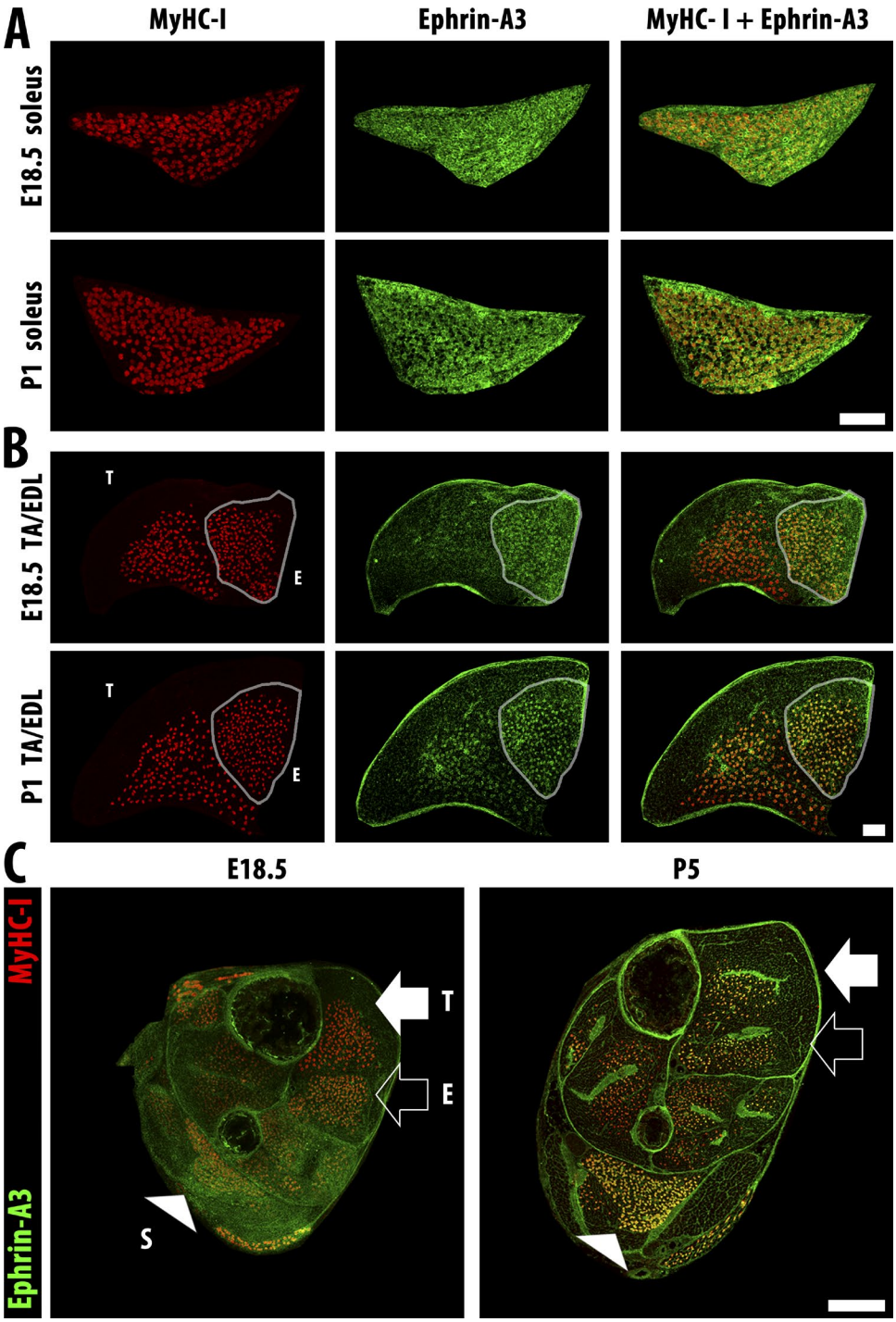

Figure 3. **Slow fibers are specified embryonically and then express ephrin-A3 after birth.** (A) Slow myofibers (MyHC-I, red) in the soleus are present at E18.5, but ephrin-A3 staining (green) remains diffuse until P1. (B) Slow myofibers (MyHC-I, red) in the EDL (outline) possess more specific ephrin-A3 (green) expression than the soleus at E18.5, but slow myofibers in the TA have only faint ephrin-A3 expression even at P1. Bars, 100 µm. (C) Transverse cryosections of distal hindlimbs of wild-type pups at E18.5 and P5 stained for ephrin-A3 (green) and MyHC-I (red) to highlight muscle-specific difference in coexpression pattern and intensity. The soleus (S, arrowhead), TA (T, closed arrow), and EDL (E, open arrow) muscles can be identified by the spatial pattern of MyHC-I^{+ve} myofibers in each section. Bar, 500 µm.

the number of slow myofibers in the anterior (electroporated) region at 28 d postcrush (Fig. 5 A, bottom).

When the number of MyHC-I^{+ve} myofibers was quantified in each treatment and compared with unelectroporated, uninjured TA muscles, no treatment produced a significant difference in the absence of nerve crush (Fig. 5 B, top), nor did electroporation with a control plasmid promote an increase in slow fibers even with denervation (Fig. 5 B, bottom, red bars). However, denervated muscles misexpressing ephrin-A3 have an eightfold increase in slow, MyHC-I^{+ve} myofibers in the anterior medial quadrant and a fivefold increase in the anterior lateral quadrant (Fig. 5 B, bottom, blue bars). In the posterior

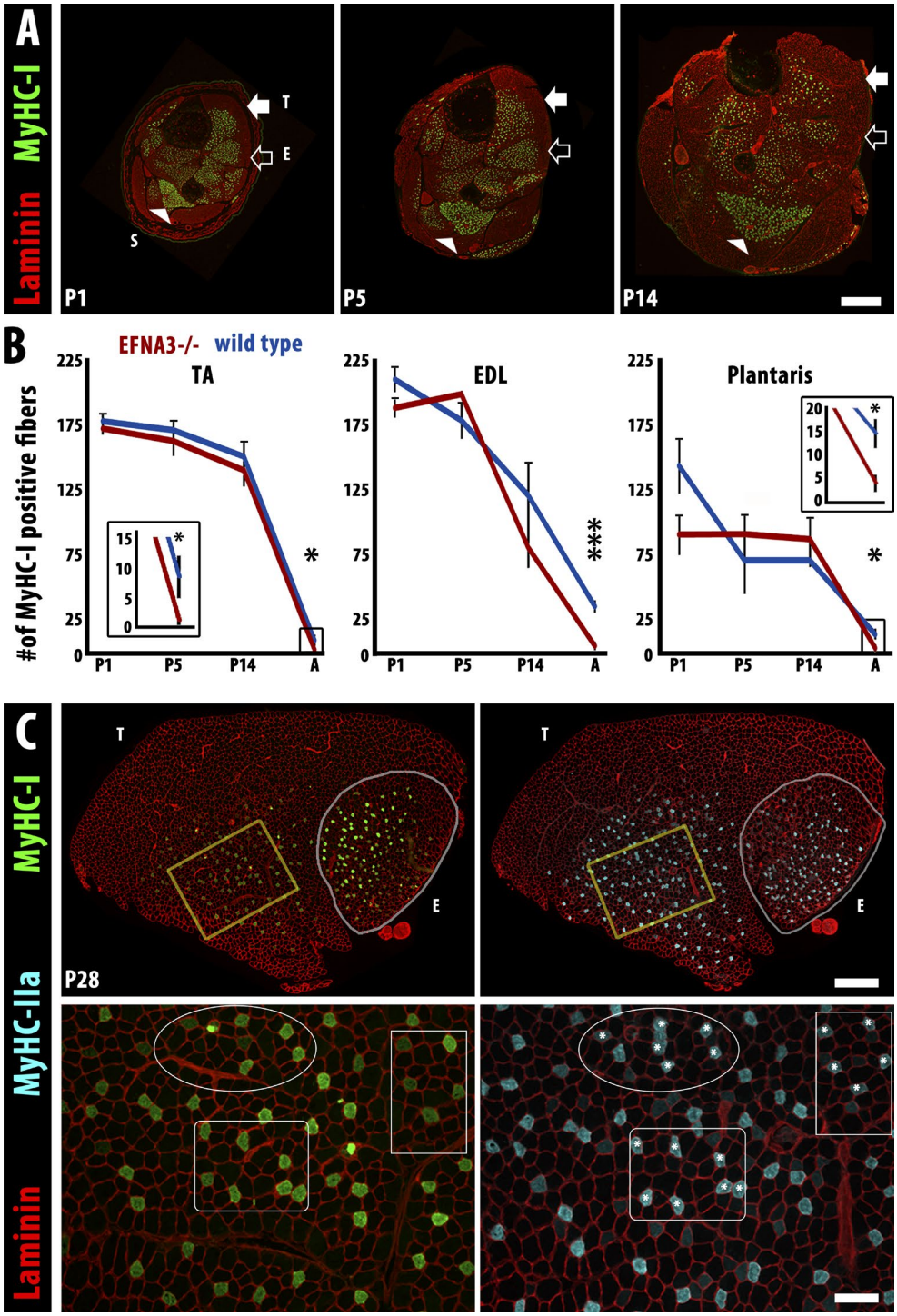

Figure 4. **The loss of slow myofibers in ephrin-A3$^{-/-}$ mice occurs postnatally by conversion to IIA fast myofibers.** (A) Immunohistochemistry showing laminin (red) and MyHC-I (green) expression in transverse cryosections of distal hindlimbs of ephrin-A3$^{-/-}$ mice at P1, P5, and P14. The soleus (S, arrowhead), TA (T, closed arrow), and EDL (E, open arrow) muscles can be identified by the spatial pattern of MyHC-I^{+ve} myofibers in each section. Bar, 500 µm. (B) Slow myofiber number in TA, EDL, and plantaris of wild-type and ephrin-A3$^{-/-}$ (EFNA3$^{-/-}$) muscles are not significantly different until after at least 2 wk of postnatal life (insets show slow myofiber number in adult TA and plantaris at a different scale). Error bars = SEM. *, $P < 0.05$; ***, $P < 0.001$. (C) MyHC-I^{+ve} myofibers in ephrin-A3$^{-/-}$ muscle sections at P28 (green, left) frequently coexpress MyHC-IIa (cyan, right), indicating that they are in transition to a faster fiber type; laminin (red) outlines myofibers on both sides. Insets (yellow boxes) are magnified under each panel: three regions are identified in each inset to facilitate comparison, and asterisks indicate MyHC-IIa^{+ve} myofibers that are also MyHC-I^{+ve}. Bars: (montages) 500 µm; (insets) 100 µm.

medial quadrant, which was not in the electroporated region but where all of the slow fibers that would normally be present in the TA are located, there was a noticeable but not significant decrease in MyHC-I^{+ve}, ephrin-A3^{+ve} myofibers in the ephrin-3 electroporated and denervated animals, whereas in the posterior lateral quadrant (which was not in the electroporated region and where there would normally be no slow myofibers), there was no change.

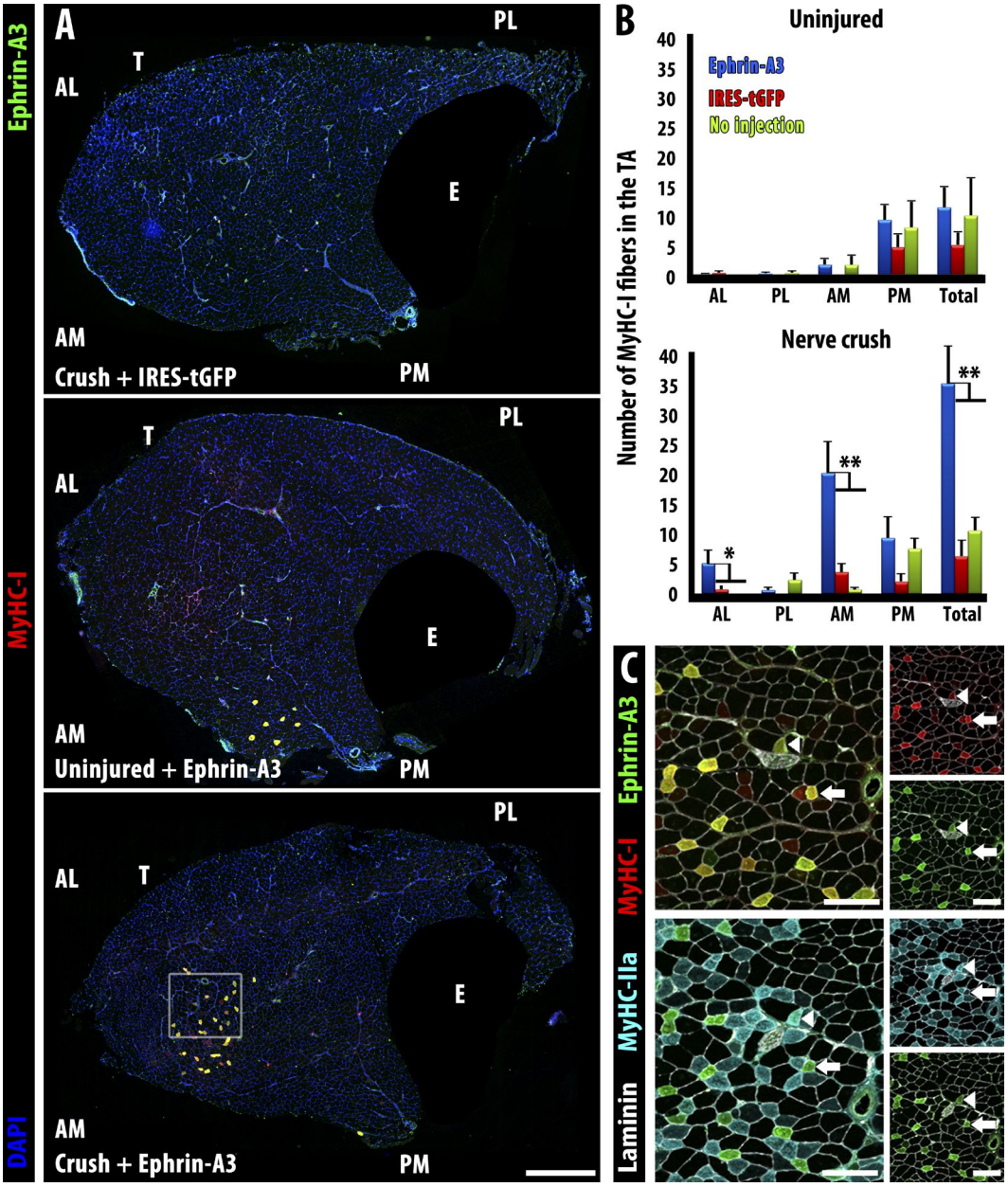

Figure 5. **Misexpression of ephrin-A3 in the TA by electroporation followed by sciatic nerve crush imposes a fast to slow fiber type switch by 28 d post-crush.** (A) Neither electroporation with a control plasmid (IRES-tGFP) followed by nerve crush (top) nor electroporation with ephrin-A3 plasmid without nerve crush (middle) significantly changed the number of slow myofibers in wild-type TA muscles compared with sham-operated controls. However, electroporation with ephrin-A3 plasmid followed by challenge with nerve crush led to significant conversion of fast myofibers to slow (MyHC-I^{+ve}) at the injection site (bottom). EDL (E) is masked in all panels. Bar, 500 µm. (B) Quantification of slow myofibers in different quadrants of the TA in the experiments described above: AL, anterior lateral; AM, anterior medial; PL, posterior lateral; PM, posterior medial. Plasmid DNA was injected into the anterior aspect of the TA followed by electroporation. Only electroporation with ephrin-A3 in conjunction with nerve crush (blue bars, bottom) significantly increases MyHC-I^{+ve} myofibers. Error bars = SEM. *, $P < 0.05$; **, $P < 0.01$. (C) Serial sections corresponding to inset box in A showing coexpression of ephrin-A3 (green) with either MyHC-I (red, top) or MyHC-IIa (cyan, bottom). Laminin is shown in white. All ephrin-A3^{+ve} myofibers express MyHC-I (i.e., arrows); a few (arrowheads) express both MyHC-I and MyHC-IIa. Bars, 100 µm. T, TA; E, EDL.

Typically, MyHC expression after denervation tends to favor MyHC-IIa as slow myofibers become faster and fast myofibers become slower (Ciciliot and Schiaffino, 2010). Costaining for fast MyHC-IIa indicates that each converted myofiber is in a variable state of transition ranging from a completely slow, ephrin-A3^{+ve} myofiber (Fig. 5 C, arrows) to a mostly fast, ephrin-A3^{-ve} hybrid myofiber (Fig. 5 C, arrowheads). The degree of variation may reflect different times of innervation by the regenerating axon (~1–3 wk; Magill et al., 2007) and/or the original type of fast myofiber, as MyHC-IIa fibers convert more readily than MyHC-IIx fibers (Pette and Staron, 1997). Because expression of MyHC-I by a myofiber requires its innervation by a slow motor neuron (Buller et al., 1960; Ciciliot and Schiaffino, 2010), these results support the hypothesis that the same ephrin-A3–dependent mechanism used during postnatal maturation to direct innervation of autonomously specified slow myofibers by slow motor neurons may also act to preserve the slow myofiber pool during reinnervation.

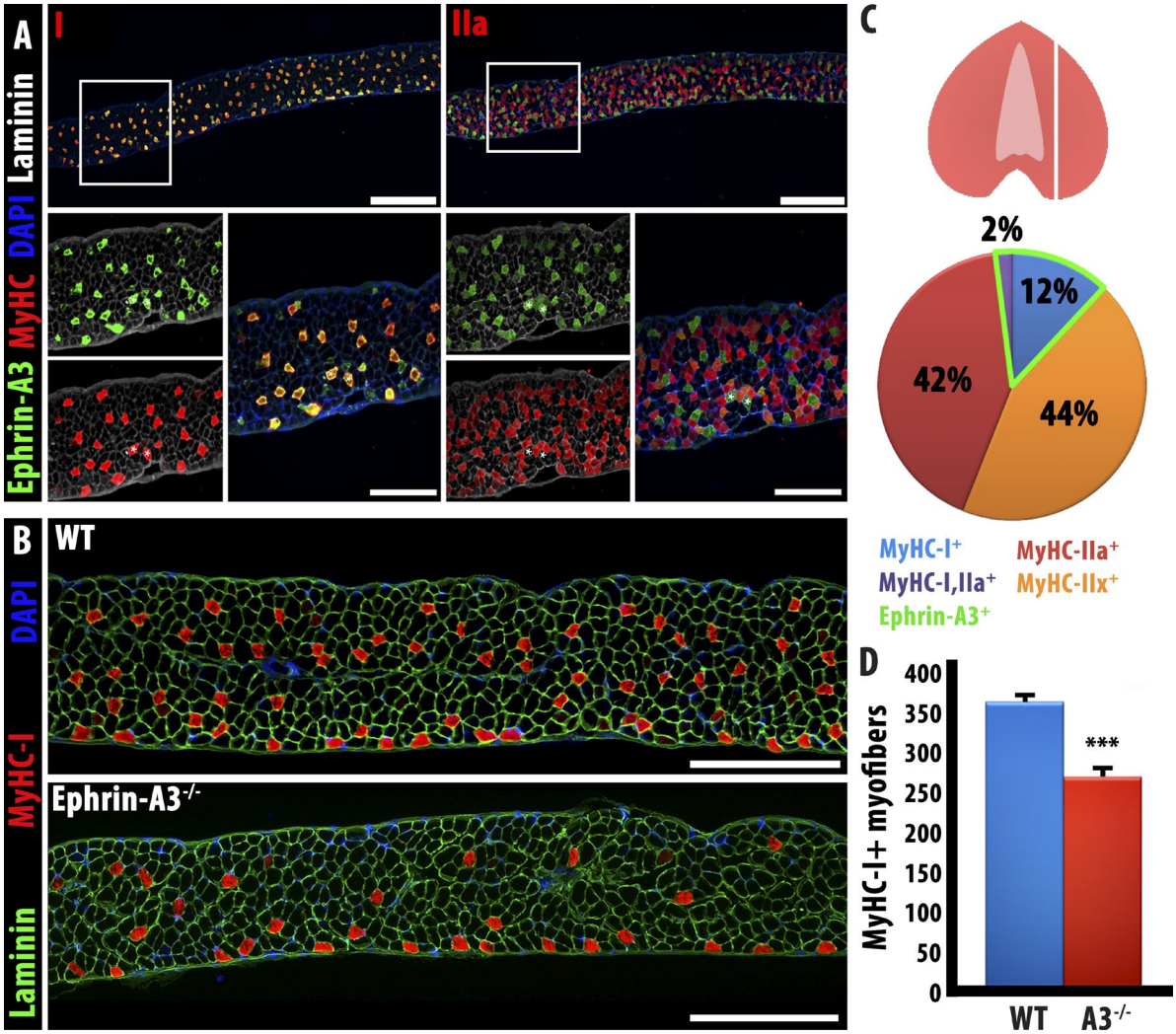

Figure 6. **Ephrin-A3$^{-/-}$ diaphragm muscle displays a phenotype intermediate between TA and soleus muscles.** (A) As noted in hindlimb muscles, ephrin-A3 expression is detected on all MyHC-I^{+ve} myofibers in the diaphragm; in sections taken as indicated in the cartoon at right, MyHC-I is expressed by 14% of myofibers scored, all of which also express ephrin-A3. Bars: (top) 400 µm; (bottom) 100 µm. (B) Equivalent sections of wild-type and ephrin-A3$^{-/-}$ adult diaphragm show a reduction, but not loss, of slow myofibers. Bars, 500 µm. (C) Representation of the plane of section in A and B and quantification of muscle fiber types and ephrin-A3 expression in WT diaphragm. (D) Quantification of Type I fibers through the same plane of section in wild-type and ephrin-A3$^{-/-}$ adult diaphragm; error bars represent SEM. WT, wild type. ***, $P < 0.001$.

Diaphragm muscle in adult ephrin-A3$^{-/-}$ mice displays an intermediate phenotype

The variability in the ephrin-A3 null phenotype between the TA/EDL (almost exclusively fast muscles, from which almost all slow myofibers are lost in the mutant) and soleus (>40% slow muscle, in which slow fiber number does not decrease in the mutant) suggested that the requirement for ephrin-A3 may be particularly acute in muscles with a relatively low intrinsic number of slow myofibers at maturity, and negligible in muscles with many slow myofibers. We therefore first surveyed ephrin-A3 expression and MyHC expression in the diaphragm, a mixed muscle with an intrinsic fraction of slow myofibers intermediate between the TA and soleus. We found that, as in hindlimb muscles, ephrin-A3 expression is limited to myofibers expressing MyHC-I, which were ∼14% of the total (Fig. 6, A and C); 2% of diaphragm myofibers coexpressed MyHC-I and MyHC-IIa, and were all ephrin-A3^{+ve}. We then compared slow myofiber number in control and ephrin-A3$^{-/-}$ diaphragms and found that there is an ∼31% decrease in slow myofiber number in the adult, an intermediate phenotype between what was observed in the TA and in the soleus (Fig. 6, B and D).

EphA8 is localized exclusively to fast motor endplates and identifies a subpopulation of terminal Schwann cells

A unique consequence of Eph/ephrin signaling is frequently the emergence of reciprocal expression patterns for ligand and receptor at steady state, so we surveyed for Eph receptors whose expression is associated specifically with fast but not slow myofibers, focusing on expression at the NMJ. Expression of ephrin ligands and Eph receptors at NMJs has been reported previously (Lai et al., 2001), although no function has been ascribed to them in this context. To identify potential cellular receptors for ephrin-A3, we screened adult NMJs (identified by acetylcholine receptor [α-bungarotoxin]) for expression of all mammalian EphA proteins. We detected EphA1, EphA2, EphA7, and EphA8; when we costained for MyHC-I to identify slow myofibers, we noted that although EphA1, EphA2, and EphA7

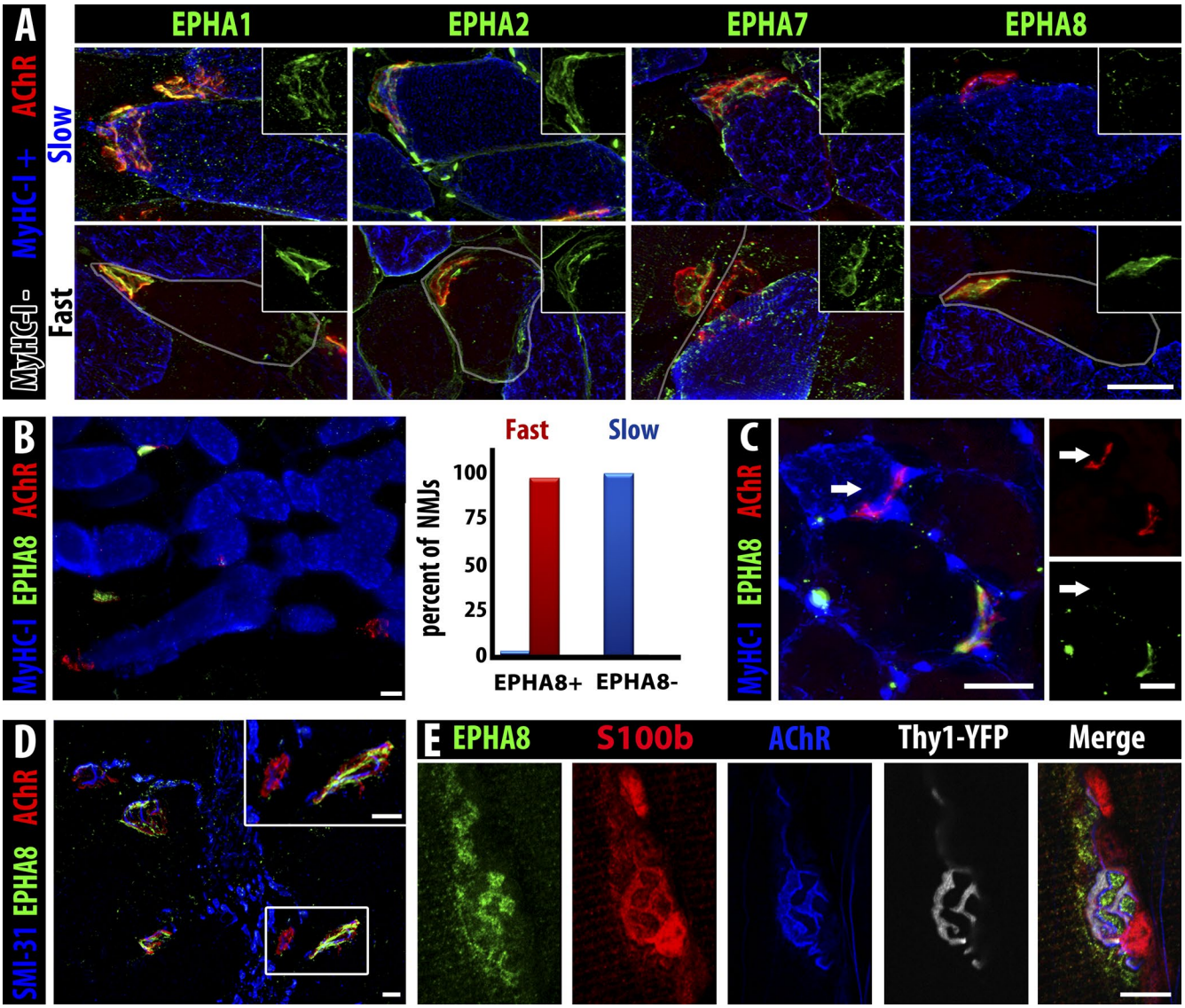

Figure 7. **EphA8 is expressed by terminal Schwann cells associated with fast myofiber NMJs.** (A) EphA1, EphA2, and EphA7 (green) are present on NMJs (α-bungarotoxin, red) of both fast myofibers (gray outline) and slow myofibers (MyHC-I, blue), but EphA8 (green, right) is only detectable at NMJs of fast myofibers. Insets show green staining for the indicated Eph at the same magnification. Bar, 25 µm. (B) Section of soleus muscle (MyHC-I^{+ve} myofibers, blue) showing expression of EphA8 (green) at fast but not slow myofiber NMJs (α-bungarotoxin, red). Bar, 25 µm. 100% of fast myofiber NMJs were positive for EphA8 (red bar), whereas almost all (97%) slow myofiber NMJs lacked EphA8 staining (blue bar); the very small fraction (<3%) of EphA8^{+ve} NMJs associated with MyHC-I^{+ve} myofibers may represent hybrid myofibers. n = 134 NMJs. (C) A fast TA myofiber converted to slow by ephrin-A3 misexpression/nerve crush does not have EphA8 at its NMJ: arrow indicates the NMJ of the same slow myofiber marked with an arrow in Fig. 5 C (all 13 converted myofibers scored were EphA8 negative). Bars, 25 µm. (D) EphA8 (green) expression is localized at the NMJ (α-bungarotoxin, red) and not associated with the motor axon (SMI-31, blue). Bars, 25 µm. α-Bungarotoxin gamma = 1.45. (E) Confocal analysis of staining for presynaptic neuron (Thy1-YFP, gray), postsynaptic myofiber (acetylcholine receptor, blue), and Schwann cell cytoplasm (S100b, red) consistent with expression of EphA8 (green) by terminal Schwann cells. Note that because S100b is cytoplasmic and EphA8 is at the cell surface, overlap of staining is not necessarily expected in these confocal sections. Bar, 10 µm.

are localized to all NMJs, EphA8 is only found at the NMJs of fast myofibers (Fig. 7, A and B) in all limb muscles surveyed (TA, EDL, soleus, and diaphragm). EphA8 is a receptor for ephrin-A3 (Park and Sánchez, 1997). We scored all identifiable NMJs in the soleus muscle for EphA8 and MyHC-I and found that that all NMJs on fast fibers (MyHC-I^{-ve}) express EphA8 (n = 81/81; Fig. 7 B). We occasionally (n = 2/53) noted NMJs of MyHC-I^{+ve} myofibers that were also positive for EphA8; these few myofibers may represent the MyHC-IIa/I hybrid population (usually ∼3% of myofibers; Pette and Staron, 2001) and/or myofibers undergoing fiber type transition.

Based on the predictions of our model, we would expect that EphA8 would be absent from the motor endplates of the fast myofibers in the TA that had been converted to slow by misexpression of ephrin-A3 followed by denervation/reinnervation. When we scored the NMJs of electroporated muscles, we found that 100% of the NMJs (n = 13/13) on the converted, slow MyHC-I^{+ve} myofibers in the TA were negative for EphA8 (Fig. 7 C; arrow indicates the NMJ of the converted myofiber labeled with an arrow in Fig. 5 C), thus demonstrating plasticity at the NMJ that corresponds to changes in MyHC and ephrin-A3 expression.

Although our initial hypothesis called for EphA8 to be expressed on the motor axon at the NMJ, further expression experiments suggested that it was not associated with the neuron itself (Fig. 7 D) but rather with a population of nonmyelinating glial cells intimately associated with the synapse, known as peripheral or terminal Schwann cells. Confocal analysis of EphA8 staining with markers for the presynaptic motor axon (Thy1-YFP), the postsynaptic myofiber (α-bungarotoxin), and Schwann cells (the small calcium-binding protein S100b) at the NMJ supported this conclusion (Fig. 7 E). Further analysis using S100b-GFP transgenic mice (Zuo et al., 2004) further validated EphA8 expression on terminal Schwann cells and potential repulsion by ephrin-A3 (Fig. S4, A–C; and Video 1 and Video 2). Although Ephs other than EphA8 have previously been localized at NMJs (Lai et al., 2001), they are expressed by the muscle fiber at the postsynaptic membrane of the NMJ rather than by any neuronal cell type, and were not described as being restricted to only a subset of NMJs. During postnatal development, we find that EphA8^{+ve} Schwann cells are already present at a majority of fast NMJs at birth and identify 100% of fast NMJs by P14 (Fig. S4, D and E), corresponding with the time frame in which axonal pruning occurs. Interestingly, a member of a different class of neuronal guidance ligands, semaphorin-3A, is also expressed during postnatal development and reinnervation on terminal Schwann cells associated with the NMJs of fast fibers, but is even more restricted than EphA8 in that it is limited to fibers expressing MyHC-IIb/x but not MyHC-IIa (De Winter et al., 2006). The mechanisms by which a subset of terminal Schwann cells up-regulate EphA8 and become associated with fast myofibers, the specific timing of their activity in matching motor neurons with appropriate fiber types, and how Eph/ephrins and other guidance molecules may guide interactions between myofibers, motor axons, and terminal Schwann cells are the subject of ongoing studies.

Discussion

Over the past several decades, multiple lines of research in avians and mammals have suggested that muscle fiber types are imposed cell-autonomously during early development (Butler et al., 1982; Condon et al., 1990); a particularly dramatic example of autonomous fiber type specification is the appearance of appropriately patterned fiber types in limb musculature that developed without innervation as a result of surgical (Condon et al., 1990) or genetic (Ashby et al., 1993) manipulation. However, the progressive emergence of postnatal motor unit homogeneity (Fladby and Jansen, 1990; Jansen and Fladby, 1990), which describes the tendency for all myofibers innervated by a single motor axon to be the same fiber type (Burke, 1999) even in muscles containing multiple fiber types in the same region (Burke and Tsairis, 1973), as well as cross-innervation (Buller et al., 1960), cross-transplantation (Gutmann and Carlson, 1975), and exogenous electrical stimulation experiments (Ausoni et al., 1990) support the idea that properties specific to the innervating neuron determine muscle fiber type in adult muscles. Intriguingly, in all cases, the efficiency by which fiber type could be externally modified was dependent on the initial fiber type composition of the muscle. Prevailing models of muscle fiber type specification thus propose that a "matching" mechanism between muscle fibers and motor axons of like types, followed by mutual adaptation, could act relatively late in development to refine and stabilize the eventual mature myofiber patterns (Donoghue and Sanes, 1994; Keller-Peck et al., 2001). Recent work that would support this mechanism includes the identification of SV2A (a synaptic vesicle protein) as a slow motor neuron marker, which becomes restricted to slow motor axons several weeks postnatally (Chakkalakal et al., 2010).

In addition, when mature myofibers lose their innervation as a result of injury to the muscle or the nerve, reinnervation occurs not only at the original site of the synapse on the muscle fiber (Marshall et al., 1977; Sanes et al., 1978) but is frequently with the same motor axon, due in large part to the continued presence of myelinated Schwann cells that had wrapped the motor axon (Ide, 1996) and the dynamic activity of nonmyelinating terminal Schwann cells that sprout after denervation and provide both growth stimulus and guidance to the regenerating axon (Reynolds and Woolf, 1992; Son and Thompson, 1995a,b; Son et al., 1996; Feng and Ko, 2007). Sanes and colleagues have demonstrated reinnervation specificity based on the rostrocaudal identity of both the muscle and the nerve (Wigston and Sanes, 1982; Donoghue et al., 1992a,b) mediated at least in part by differential expression of specific ephrins (Feng et al., 2000). There is also evidence for selective reinnervation by fiber type (Elizalde et al., 1983; Soileau et al., 1987; Thompson et al., 1987). When presented with inappropriate targets, such as in cross-reinnervation experiments, some inappropriate neuromuscular synapses can be induced to form: fast muscles are readily converted to a slow phenotype by innervation with slow motor neurons, but slow muscles are refractory to innervation by fast motor neurons and thus to fiber type switching (Nemeth and Turk, 1984; Dum et al., 1985; Dolenc et al., 1994).

Eph/ephrin interactions direct a broad variety of cellular and intercellular processes in the context of neuronal and neuromuscular development (Kao et al., 2012; Lisabeth et al., 2013; Laussu et al., 2014); the role for Eph/ephrin signaling we describe in the context of myofiber innervation thus adds to the well-known activity of these signaling molecules in motor axon repulsion (Orioli and Klein, 1997), attraction (Dudanova et al., 2012), fasciculation (Luxey et al., 2013), dorsal/ventral patterning (Luria et al., 2008), and topographic mapping (Chadaram et al., 2007). The number and variety of processes mediated by this signaling pathway often results in expression of multiple Ephs and ephrins on the same cell, where they may act cooperatively in cis (Kao and Kania, 2011), independently in trans (Feng et al., 2000), or even oppositely in trans, with opposite effects on the cell from distinct membrane compartments (Marquardt et al., 2005). A particular complication when investigating Eph/ephrin signaling is the extreme promiscuity and thus context dependence of interactions between specific ligand–receptor pairs (Noberini et al., 2012; Nikolov et al., 2013; Seiradake et al., 2013). However, the robust mutual exclusivity of ephrin-A3 and EphA8 expression we observed suggests that they may be participating in classical repulsive signaling at the NMJs of maturing slow myofibers to inhibit formation of stable synapses with fast motor neurons (Fig. 8 and Video 2), as was first proposed very shortly after the pathway was first characterized (Rafuse et al., 1996). As discussed below, this may serve to confer a competitive advantage to slow motor neurons, which otherwise are generally present in fewer numbers and form smaller motor units (Kanning et al., 2010). Our data also show that this developmental mechanism remains available during reinnervation in the adult, and thus it would also serve to explain the recapitulation of muscle fiber type after muscle or nerve injury. However,

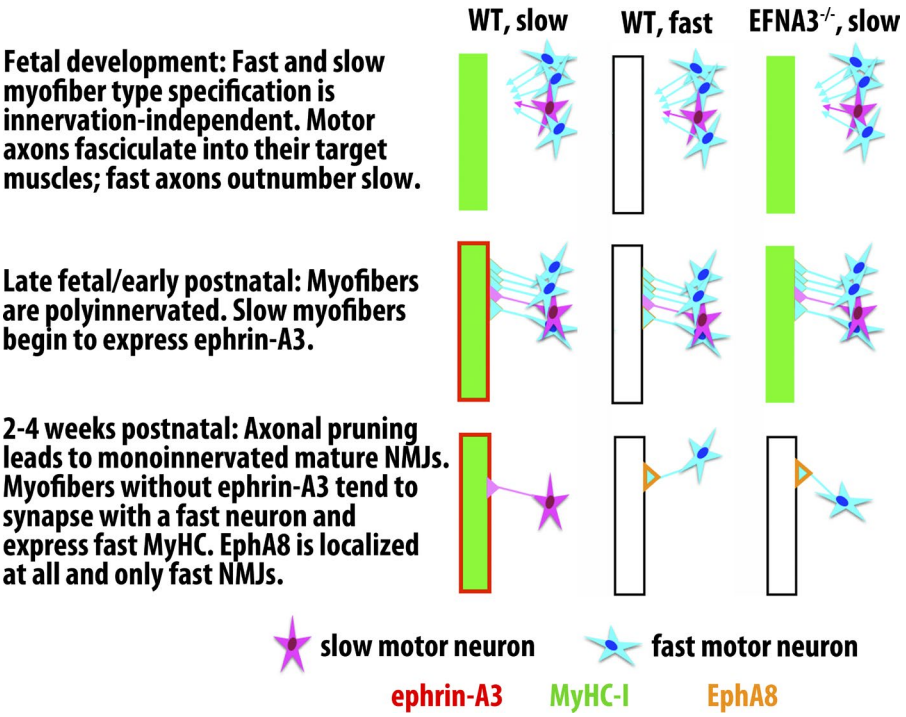

Figure 8. **Model for slow muscle fiber specification via ephrin-A3/EphA8 repulsive interactions during postnatal synaptic pruning.** We hypothesize that after cell-autonomous slow myofiber specification during embryonic and fetal development, MyHC-I–expressing myofibers begin to express ephrin-A3, leading to preferential elimination of synapses with fast motor axons late in NMJ maturation. In the absence of ephrin-A3, because fast motor axons outnumber slow motor axons in most mixed fiber type muscles, this competitive advantage is lost and the slow myofiber population is largely lost as well because of innervation-dependent fiber type switching to a faster phenotype. It is not yet clear what lineage or local signaling factors induce a subset of terminal Schwann cells to become EphA8^{+ve}, or when and how they become localized to fast NMJs, although they are present at birth and are restricted to maturing fast NMJs by P14 (Fig. S5). We therefore indicate expression of EphA8 only in the final, steady state. WT, wild type.

many pieces of the puzzle remain to be explored. Particularly intriguing is the potential involvement of terminal Schwann cells in this process. Because it has been shown that terminal Schwann cells are instrumental in both axon pruning during postnatal development (Smith et al., 2013) and guiding axonal processes back to the muscle membrane after muscle or nerve damage (Koirala et al., 2000; Kang et al., 2003), the argument for terminal Schwann cells as key players in ensuring appropriate innervation and reinnervation of fast versus slow myofibers is appealing and is currently being investigated. In addition, the de novo expression of endogenous ephrin-A3 by fast myofibers converted to slow by innervation with a slow motor axon (as in our misexpression/crush experiments) suggests that transcription of MyHC-I and ephrin-A3 may be transcriptionally linked in adult myofibers, although they do not appear to be during prenatal muscle development. The mechanism by which this absolute correlation of expression emerges may shed additional light on fiber type–specific gene expression, as well as potential distinctions between cell-autonomous and innervation-dependent fiber type specification.

The divergence of the ephrin-A3$^{-/-}$ phenotype in the soleus from that in other hindlimb muscles is also intriguing. On the one hand, it could imply that different mechanisms for pairing myofibers with motor neurons exist in different muscles, which would significantly increase the complexity of the system and require an even more cell-autonomous direction of patterning. Alternately, a sufficient variation in inputs could result in different outputs even with the same mechanism, i.e., the number of slow neurons available to innervate the soleus may simply be large enough to not require the competitive advantage conferred by ephrin-A3 in other mixed muscles such as the TA or EDL, where the great majority of motor axons would be fast, or the gastrocnemius, which has distinct regions enriched in slow myofibers. This would be consistent with existing studies such as the work of Rafuse and Landmesser (Rafuse et al., 1996) showing that intrinsically different pools of motor neurons project to muscles that are predominantly fast versus muscles composed of mixed fast and slow, followed by fiber type–specific formation of NMJs. It is also supported by our study of the diaphragm, a mixed muscle with a slow myofiber representation intermediate between the TA and soleus, which displays a phenotype in the ephrin-A3$^{-/-}$ mice that is also intermediate between the TA and soleus. It is important to note that, as in many other developmental contexts in which Eph/ephrin signaling mediates cell sorting or boundary formation, in our model ephrin-A3 is not required for slow myofiber specification either cell-autonomously or non–cell-autonomously, but rather functions to prevent their inappropriate innervation and specification as fast myofibers by fast motor axons. Thus, the TA and the soleus anchor opposite ends of a spectrum from minimally slow (ephrin-A3 is required to preserve slow myofiber identity) to maximally slow (ephrin-A3 is dispensable for slow myofiber identity) with the diaphragm occupying the middle ground in prevalence of slow myofiber specification as well as penetrance of the ephrin-A3$^{-/-}$ phenotype.

The absolute correlation of ephrin-A3 expression with MyHC-I raises the question of what is occurring during physiological fiber type shifts, such as during training or aging/disease. It is possible that acquired or induced changes in MyHC expression in the myofiber could lead to accompanying changes in guidance molecule expression, destabilizing the synapse and permitting new interactions with motor axons of a different type; this would be consistent with data showing that the prevalence of the slow motor axon marker SV2A increases in muscles pushed to a slower phenotype by overexpression of PGC-1α (Chakkalakal et al., 2012). It is also possible that retrograde signals are transduced from the muscle via guidance molecule signaling, leading to a change in the motor neuron's firing frequency and guidance molecule expression. Further analysis of both wild-type and ephrin-A3$^{-/-}$ mutant mice in the context of aging, training, and disease should prove informative in refining and expanding this model.

Materials and methods

Animal care and use

All mice were handled in accordance with National Institutes of Health– and Institutional Animal Care and Use Committee–approved protocols. Female age-matched ephrin-A3 nontransgenic C57BL/6 mice were the control for female ephrin-A3$^{-/-}$ mice. Female B6D2F1 mice (The Jackson Laboratory) were used for in vivo electroporation. S100-GFP mice were the gift of A. Snyder-Warwick (Washington University in St. Louis, St. Louis, MO).

Immunohistochemistry and imaging

Immunohistochemistry and imaging for all panels except Fig. 7 E were done as previously described (Stark et al., 2011). Note that, although immunopositivity for ephrin-A3 can extend to the myofiber cytoplasm as well as the membrane, this is consistent with our prior published data (Stark et al., 2011) as well as with published results in other cell types using this ephrin-A3 antibody (Stadler et al., 2001; de Saint-Vis et al., 2003; Fasanaro et al., 2008; Jiao et al., 2008). Additional validation of antibody specificity is provided in Fig. S5. Concentrations of primary antibodies (Santa Cruz Biotechnology, Inc. unless otherwise noted) were rabbit anti–ephrin-A3, 1:300; rabbit anti-EphA1, 2, 7, and 8, 1:100; rabbit anti-laminin, 1:400 (Sigma-Aldrich); mouse anti-neurofilament 1:1,000 (SMI-31; Covance); and mouse anti–MyHC-I, -IIa, and -IIb (clones BA-D5, SC-71, and BF-F3; Developmental Studies Hybridoma Bank), 1:50. Acetylcholine receptors were stained with TRITC-conjugated α-bungarotoxin 1:1,000 (Invitrogen). Images were collected on an upright microscope (BX-61; Olympus) with UPlanFL N objectives (0.50 NA) using a charge-coupled device camera (Retiga; QImaging) under ambient conditions. μManager software (www.micro-manager.org) was used to run the microscope and Photoshop CS4 software (Adobe) was used to merge and montage each image. All constrained iterative deconvolution and 3D reconstruction was done with AxioVision software, version 4.8 (Carl Zeiss).

For the confocal images in Fig. 7 E, EDL muscles from adult (90 d old) female Thy1-YFP mice (The Jackson Laboratory) were dissected under oxygenated (95% O_2 and 5% CO_2) Rees' Ringer's solution (110-mM NaCl, 5-mM KCl, 1-mM $MgCl_2$, 25-mM $NaHCO_3$, 2-mM $CaCl_2$, 11-mM glucose, 0.3-mM glutamate, 0.4-mM glutamine, 5-mM balanced electrolyte solution, 4.34×10^{-7}-mM cocarboxylase, and 0.036-mM choline chloride, pH 7.3), then pinned in Sylgard-coated Petri dishes and fixed for 10 min in 4% formaldehyde at room temperature, and permeabilized in 100% cold methanol for 6 min at −20°C. Nonspecific labeling was minimized by incubating the muscles in a solution of 10% normal donkey serum and 0.01% Triton X-100 for 20 min.

To avoid cross-reactivity of the EphA8 (H70) and the S100b antibodies (both raised in rabbit), muscles were incubated overnight at 4°C with anti-EphA8, rinsed, and then incubated with goat anti–rabbit IgG (H+L) Fab fragments (10 μg/ml; 111-007-003; Jackson ImmunoResearch Laboratories, Inc.) for 60 min at RT. The first secondary antibody, Alexa Fluor 594 donkey anti–goat IgG (H+L; 1:500; A110558; Invitrogen), was applied for 60 min at RT. Preparations were then incubated with rabbit anti-S100b (1:250; Z0311; Dako) for 60 min at RT to label terminal Schwann cells and then with Alexa Fluor 647 donkey anti-rabbit (1:500; 711-605-152; Jackson ImmunoResearch Laboratories, Inc.) for 60 min at RT. Finally, to label nicotinic acetylcholine receptors, muscles were incubated with 4 μg/ml α-bungarotoxin (CF405s; Biotium) for 45 min at RT. All antibodies were prepared in a 2% normal donkey serum/PBS/0.01% Triton X-100 solution. Muscles were rinsed with PBS containing 0.01% Triton X-100 (three times for 5 min each) in between each antibody incubation. After the final wash, preparations were mounted in Prolong Diamond (Invitrogen).

Image acquisition was done using a scanning confocal microscope (FV1000; Olympus) equipped with a 60× oil immersion objective (1.42 NA). Images were acquired at a resolution of 640 × 640 pixels with a dwell time of 8 μs per pixel. Images were acquired at a zoom factor of 2.5×, and a Kalman filter (two) was performed to minimize the noise level. The aperture of the pinhole of the confocal system was set at its minimal value of 100 μm. The four labels were simultaneously imaged using the following configuration of the virtual channels. Channel 1: the excitation light was passed through a set of three dichroic mirrors, and detection of the emitted fluorescent light was achieved using three independent photomultiplier tubes, two of which were equipped with spectral detectors and the third one with a set of dichroic and emission filters (SDM560, band pass of 500–545 nm; SDM640, band pass of 570–625 nm and a barrier filter BA 655–755 nm). Three independent laser lines were used: the 488-nm line of an argon laser with a power output set at 8%, a 559-nm diode laser with the power output set at 17%, and a 635-nm diode laser with a power output set at 8%. Channel 2: the 405-nm diode excitation light was passed through a set of two dichroic mirrors (DM405/488), and detection of the emitted fluorescent light was achieved using a 425–475-nm spectral window.

In vivo electroporation and sciatic nerve crush

Ephrin-A3 cDNA was subcloned into the pCMV6-AC-IRES-tGFP backbone (OriGene). Fur on the TA was removed and 20 μg of 1 mg/ml plasmid was injected i.m., and then six 55-ms pulses of 100 V were applied with each polarity (12 total). 3 d after electroporation, the sciatic nerve was crushed with fine forceps (three times for 3 s each). Recovery was allowed for 21 or 28 d before removing the TA for analysis. To quantify the change in fiber type, we divided the TA into quadrants. Electroporation had been targeted to the anterior of the muscle (anterior lateral and anterior medial), and posterior lateral and posterior medial were also scored to control for the endogenous slow myofiber population typically located in the posterior medial region. All myofibers scoring positive for slow MyHC-I in each quadrant were counted.

Statistical analysis

Muscles from a minimum of three mice were used for fiber type quantification. A one-tailed Student's *t* test for two samples of equal variance was used to calculate p-values.

Online supplemental material

Fig. S1 shows fast IIa and IIb myofiber distribution in ephrin-A3$^{-/-}$ muscles. Fig. S2 shows ephrin-A3 expression during limb muscle development. Fig. S3 shows the in vivo electroporation/nerve crush procedure. Fig. S4 shows ephrin-A3 repulsion by S100b-GFP–labeled Schwann cells and EphA8 expression during postnatal development, and Fig. S5 shows specificity testing of anti–ephrin-A3. Z-stack imaging of EphA8 expression on an S100b-GFP–labeled terminal Schwann cell is available as Video 1, and time-lapse imaging of S100b-GFP–labeled cells on ephrin-A3-Fc stripes is available as Video 2. Online supplemental material is available at http://www.jcb.org/cgi/content/full/jcb.201502036/DC1.

Acknowledgments

This work was funded by National Institutes of Health grants AR056814 and AR067450 to DDW Cornelison.

S100-GFP mice were the gift of Dr. Alison Snyder-Warwick. The authors thank John Dirnberger for image processing support.

The authors declare no competing financial interests.

Author contributions: D.A. Stark designed and performed the experiments and drafted the manuscript. N.J. Coffey analyzed diaphragm muscle. L.L. Arnold, H.R. Pancoast, and J.P.D. Walker assisted in experimental procedures and analysis. J. Vallée and R. Robitaille performed confocal analysis of terminal Schwann cells. M.L. Garcia provided training and assistance for sciatic nerve crush experiments. DDW Cornelison supervised the experimental design, performance, and data analysis and produced the final manuscript.

Submitted: 9 February 2015
Accepted: 22 October 2015

References

Agbulut, O., P. Noirez, F. Beaumont, and G. Butler-Browne. 2003. Myosin heavy chain isoforms in postnatal muscle development of mice. *Biol. Cell.* 95:399–406. http://dx.doi.org/10.1016/S0248-4900(03)00087-X

Aihara, H., and J. Miyazaki. 1998. Gene transfer into muscle by electroporation in vivo. *Nat. Biotechnol.* 16:867–870. http://dx.doi.org/10.1038/nbt0998-867

Ashby, P.R., S.J. Wilson, and A.J. Harris. 1993. Formation of primary and secondary myotubes in aneural muscles in the mouse mutant peroneal muscular atrophy. *Dev. Biol.* 156:519–528. http://dx.doi.org/10.1006/dbio.1993.1098

Augusto, V., C.R. Padovani, and G.E.R. Campos. 2004. Skeletal muscle fiber types in C57BL6 mice. *Braz. J. Morphol. Sci.* 21:89–94.

Ausoni, S., L. Gorza, S. Schiaffino, K. Gundersen, and T. Lømo. 1990. Expression of myosin heavy chain isoforms in stimulated fast and slow rat muscles. *J. Neurosci.* 10:153–160.

Buller, A.J., J.C. Eccles, and R.M. Eccles. 1960. Interactions between motoneurones and muscles in respect of the characteristic speeds of their responses. *J. Physiol.* 150:417–439. http://dx.doi.org/10.1113/jphysiol.1960.sp006395

Burke, R.E. 1999. Revisiting the notion of 'motor unit types'. *Prog. Brain Res.* 123:167–175. http://dx.doi.org/10.1016/S0079-6123(08)62854-X

Burke, R.E., and P. Tsairis. 1973. Anatomy and innervation ratios in motor units of cat gastrocnemius. *J. Physiol.* 234:749–765. http://dx.doi.org/10.1113/jphysiol.1973.sp010370

Butler, J., E. Cosmos, and J. Brierley. 1982. Differentiation of muscle fiber types in aneurogenic brachial muscles of the chick embryo. *J. Exp. Zool.* 224:65–80. http://dx.doi.org/10.1002/jez.1402240108

Carmona, M.A., K.K. Murai, L. Wang, A.J. Roberts, and E.B. Pasquale. 2009. Glial ephrin-A3 regulates hippocampal dendritic spine morphology and glutamate transport. *Proc. Natl. Acad. Sci. USA.* 106:12524–12529. http://dx.doi.org/10.1073/pnas.0903328106

Chadaram, S.R., M.B. Laskowski, and R.D. Madison. 2007. Topographic specificity within membranes of a single muscle detected in vitro. *J. Neurosci.* 27:13938–13948. http://dx.doi.org/10.1523/JNEUROSCI.3055-07.2007

Chakkalakal, J.V., H. Nishimune, J.L. Ruas, B.M. Spiegelman, and J.R. Sanes. 2010. Retrograde influence of muscle fibers on their innervation revealed by a novel marker for slow motoneurons. *Development.* 137:3489–3499. http://dx.doi.org/10.1242/dev.053348

Chakkalakal, J.V., S. Kuang, M. Buffelli, J.W. Lichtman, and J.R. Sanes. 2012. Mouse transgenic lines that selectively label Type I, Type IIA, and Types IIX+B skeletal muscle fibers. *Genesis.* 50:50–58. http://dx.doi.org/10.1002/dvg.20794

Ciciliot, S., and S. Schiaffino. 2010. Regeneration of mammalian skeletal muscle. Basic mechanisms and clinical implications. *Curr. Pharm. Des.* 16:906–914. http://dx.doi.org/10.2174/138161210790883453

Condon, K., L. Silberstein, H.M. Blau, and W.J. Thompson. 1990. Differentiation of fiber types in aneural musculature of the prenatal rat hindlimb. *Dev. Biol.* 138:275–295. http://dx.doi.org/10.1016/0012-1606(90)90197-Q

de Saint-Vis, B., C. Bouchet, G. Gautier, J. Valladeau, C. Caux, and P. Garrone. 2003. Human dendritic cells express neuronal Eph receptor tyrosine kinases: role of EphA2 in regulating adhesion to fibronectin. *Blood.* 102:4431–4440. http://dx.doi.org/10.1182/blood-2003-02-0500

De Winter, F., T. Vo, F.J. Stam, L.A. Wisman, P.R. Bär, S.P. Niclou, F.L. van Muiswinkel, and J. Verhaagen. 2006. The expression of the chemorepellent Semaphorin 3A is selectively induced in terminal Schwann cells of a subset of neuromuscular synapses that display limited anatomical plasticity and enhanced vulnerability in motor neuron disease. *Mol. Cell. Neurosci.* 32:102–117. http://dx.doi.org/10.1016/j.mcn.2006.03.002

Dolenc, I., N. Crne-Finderle, I. Erzen, and J. Sketelj. 1994. Satellite cells in slow and fast rat muscles differ in respect to acetylcholinesterase regulation mechanisms they convey to their descendant myofibers during regeneration. *J. Neurosci. Res.* 37:236–246. http://dx.doi.org/10.1002/jnr.490370209

Donoghue, M.J., and J.R. Sanes. 1994. All muscles are not created equal. *Trends Genet.* 10:396–401. http://dx.doi.org/10.1016/0168-9525(94)90056-6

Donoghue, M.J., R. Morris-Valero, Y.R. Johnson, J.P. Merlie, and J.R. Sanes. 1992a. Mammalian muscle cells bear a cell-autonomous, heritable memory of their rostrocaudal position. *Cell.* 69:67–77. http://dx.doi.org/10.1016/0092-8674(92)90119-W

Donoghue, M.J., B.L. Patton, J.R. Sanes, and J.P. Merlie. 1992b. An axial gradient of transgene methylation in murine skeletal muscle: genomic imprint of rostrocaudal position. *Development.* 116:1101–1112.

Donoghue, M.J., J.P. Merlie, and J.R. Sanes. 1996. The Eph kinase ligand AL-1 is expressed by rostral muscles and inhibits outgrowth from caudal neurons. *Mol. Cell. Neurosci.* 8:185–198. http://dx.doi.org/10.1006/mcne.1996.0056

Dudanova, I., T.J. Kao, J.E. Herrmann, B. Zheng, A. Kania, and R. Klein. 2012. Genetic evidence for a contribution of EphA:ephrinA reverse signaling to motor axon guidance. *J. Neurosci.* 32:5209–5215. http://dx.doi.org/10.1523/JNEUROSCI.5707-11.2012

Dum, R.P., M.J. O'Donovan, J. Toop, and R.E. Burke. 1985. Cross-reinnervated motor units in cat muscle. I. Flexor digitorum longus muscle units reinnervated by soleus motoneurons. *J. Neurophysiol.* 54:818–836.

Elizalde, A., M. Huerta, and E. Stefani. 1983. Selective reinnervation of twitch and tonic muscle fibres of the frog. *J. Physiol.* 340:513–524. http://dx.doi.org/10.1113/jphysiol.1983.sp014777

Emerson, C.P., and S.D. Hauschka. 2004. Embryonic origins of skeletal muscles. *In* Myology, Basic and Clinical. A.G. Engel and C. Franzini-Armstrong, editors. McGraw-Hill Inc., New York. 3–44.

Fasanaro, P., Y. D'Alessandra, V. Di Stefano, R. Melchionna, S. Romani, G. Pompilio, M.C. Capogrossi, and F. Martelli. 2008. MicroRNA-210 modulates endothelial cell response to hypoxia and inhibits the receptor tyrosine kinase ligand Ephrin-A3. *J. Biol. Chem.* 283:15878–15883. http://dx.doi.org/10.1074/jbc.M800731200

Feng, Z., and C.P. Ko. 2007. Neuronal glia interactions at the vertebrate neuromuscular junction. *Curr. Opin. Pharmacol.* 7:316–324. http://dx.doi.org/10.1016/j.coph.2006.12.003

Feng, G., M.B. Laskowski, D.A. Feldheim, H. Wang, R. Lewis, J. Frisen, J.G. Flanagan, and J.R. Sanes. 2000. Roles for ephrins in positionally selective synaptogenesis between motor neurons and muscle fibers. *Neuron.* 25:295–306. http://dx.doi.org/10.1016/S0896-6273(00)80895-8

Fladby, T., and J.K. Jansen. 1990. Development of homogeneous fast and slow motor units in the neonatal mouse soleus muscle. *Development.* 109:723–732.

Garnett, R.A., M.J. O'Donovan, J.A. Stephens, and A. Taylor. 1979. Motor unit organization of human medial gastrocnemius. *J. Physiol.* 287:33–43. http://dx.doi.org/10.1113/jphysiol.1979.sp012643

Gunning, P., and E. Hardeman. 1991. Multiple mechanisms regulate muscle fiber diversity. *FASEB J.* 5:3064–3070.

Gutmann, E., and B.M. Carlson. 1975. Contractile and histochemical properties of regenerating cross-transplanted fast and slow muscles in the rat. *Pflugers Arch.* 353:227–239. http://dx.doi.org/10.1007/BF00584286

Hamm, T.M., P.M. Nemeth, L. Solanki, D.A. Gordon, R.M. Reinking, and D.G. Stuart. 1988. Association between biochemical and physiological properties in single motor units. *Muscle Nerve.* 11:245–254. http://dx.doi.org/10.1002/mus.880110309

Harris, A.J., R.B. Fitzsimons, and J.C. McEwan. 1989. Neural control of the sequence of expression of myosin heavy chain isoforms in foetal mammalian muscles. *Development.* 107:751–769.

Ide, C. 1996. Peripheral nerve regeneration. *Neurosci. Res.* 25:101–121. http://dx.doi.org/10.1016/0168-0102(96)01042-5

Iwamasa, H., K. Ohta, T. Yamada, K. Ushijima, H. Terasaki, and H. Tanaka. 1999. Expression of Eph receptor tyrosine kinases and their ligands in chick embryonic motor neurons and hindlimb muscles. *Dev. Growth Differ.* 41:685–698. http://dx.doi.org/10.1046/j.1440-169x.1999.00468.x

Jansen, J.K., and T. Fladby. 1990. The perinatal reorganization of the innervation of skeletal muscle in mammals. *Prog. Neurobiol.* 34:39–90. http://dx.doi.org/10.1016/0301-0082(90)90025-C

Jiao, J.W., D.A. Feldheim, and D.F. Chen. 2008. Ephrins as negative regulators of adult neurogenesis in diverse regions of the central nervous system. *Proc. Natl. Acad. Sci. USA.* 105:8778–8783. http://dx.doi.org/10.1073/pnas.0708861105

Kang, H., L. Tian, and W. Thompson. 2003. Terminal Schwann cells guide the reinnervation of muscle after nerve injury. *J. Neurocytol.* 32:975–985. http://dx.doi.org/10.1023/B:NEUR.0000020636.27222.2d

Kanning, K.C., A. Kaplan, and C.E. Henderson. 2010. Motor neuron diversity in development and disease. *Annu. Rev. Neurosci.* 33:409–440. http://dx.doi.org/10.1146/annurev.neuro.051508.135722

Kao, T.J., and A. Kania. 2011. Ephrin-mediated cis-attenuation of Eph receptor signaling is essential for spinal motor axon guidance. *Neuron.* 71:76–91. http://dx.doi.org/10.1016/j.neuron.2011.05.031

Kao, T.J., C. Law, and A. Kania. 2012. Eph and ephrin signaling: Lessons learned from spinal motor neurons. *Semin. Cell Dev. Biol.* 23:83–91. http://dx.doi.org/10.1016/j.semcdb.2011.10.016

Kardon, G., J.K. Campbell, and C.J. Tabin. 2002. Local extrinsic signals determine muscle and endothelial cell fate and patterning in the vertebrate limb. *Dev. Cell.* 3:533–545. http://dx.doi.org/10.1016/S1534-5807(02)00291-5

Keller-Peck, C.R., M.K. Walsh, W.B. Gan, G. Feng, J.R. Sanes, and J.W. Lichtman. 2001. Asynchronous synapse elimination in neonatal motor units: studies using GFP transgenic mice. *Neuron.* 31:381–394. http://dx.doi.org/10.1016/S0896-6273(01)00383-X

Koirala, S., H. Qiang, and C.P. Ko. 2000. Reciprocal interactions between perisynaptic Schwann cells and regenerating nerve terminals at the frog neuromuscular junction. *J. Neurobiol.* 44:343–360. http://dx.doi.org/10.1002/1097-4695(20000905)44:3<343::AID-NEU5>3.0.CO;2-O

Krull, C.E., R. Lansford, N.W. Gale, A. Collazo, C. Marcelle, G.D. Yancopoulos, S.E. Fraser, and M. Bronner-Fraser. 1997. Interactions of Eph-related receptors and ligands confer rostrocaudal pattern to trunk neural crest migration. *Curr. Biol.* 7:571–580. http://dx.doi.org/10.1016/S0960-9822(06)00256-9

Lai, K.O., F.C. Ip, J. Cheung, A.K. Fu, and N.Y. Ip. 2001. Expression of Eph receptors in skeletal muscle and their localization at the neuromuscular junction. *Mol. Cell. Neurosci.* 17:1034–1047. http://dx.doi.org/10.1006/mcne.2001.0997

Laussu, J., A. Khuong, J. Gautrais, and A. Davy. 2014. Beyond boundaries—Eph:ephrin signaling in neurogenesis. *Cell Adhes. Migr.* 8:349–359. http://dx.doi.org/10.4161/19336918.2014.969990

Lisabeth, E.M., G. Falivelli, and E.B. Pasquale. 2013. Eph receptor signaling and ephrins. *Cold Spring Harb. Perspect. Biol.* 5: a009159. http://dx.doi.org/10.1101/cshperspect.a009159

Luria, V., D. Krawchuk, T.M. Jessell, E. Laufer, and A. Kania. 2008. Specification of motor axon trajectory by ephrin-B:EphB signaling: symmetrical control of axonal patterning in the developing limb. *Neuron.* 60:1039–1053. http://dx.doi.org/10.1016/j.neuron.2008.11.011

Luxey, M., T. Jungas, J. Laussu, C. Audouard, A. Garces, and A. Davy. 2013. Eph:ephrin-B1 forward signaling controls fasciculation of sensory and motor axons. *Dev. Biol.* 383:264–274. http://dx.doi.org/10.1016/j.ydbio.2013.09.010

Magill, C.K., A. Tong, D. Kawamura, A. Hayashi, D.A. Hunter, A. Parsadanian, S.E. Mackinnon, and T.M. Myckatyn. 2007. Reinnervation of the tibialis anterior following sciatic nerve crush injury: a confocal microscopic study in transgenic mice. *Exp. Neurol.* 207:64–74. http://dx.doi.org/10.1016/j.expneurol.2007.05.028

Marquardt, T., R. Shirasaki, S. Ghosh, S.E. Andrews, N. Carter, T. Hunter, and S.L. Pfaff. 2005. Coexpressed EphA receptors and ephrin-A ligands mediate opposing actions on growth cone navigation from distinct membrane domains. *Cell.* 121:127–139. http://dx.doi.org/10.1016/j.cell.2005.01.020

Marshall, L.M., J.R. Sanes, and U.J. McMahan. 1977. Reinnervation of original synaptic sites on muscle fiber basement membrane after disruption of the muscle cells. *Proc. Natl. Acad. Sci. USA.* 74:3073–3077. http://dx.doi.org/10.1073/pnas.74.7.3073

Milner, L.D., V.F. Rafuse, and L.T. Landmesser. 1998. Selective fasciculation and divergent pathfinding decisions of embryonic chick motor axons projecting to fast and slow muscle regions. *J. Neurosci.* 18:3297–3313.

Nemeth, P.M., and W.R. Turk. 1984. Biochemistry of rat single muscle fibres in newly assembled motor units following nerve crush. *J. Physiol.* 355:547–555. http://dx.doi.org/10.1113/jphysiol.1984.sp015437

Nemeth, P.M., D. Pette, and G. Vrbová. 1981. Comparison of enzyme activities among single muscle fibres within defined motor units. *J. Physiol.* 311:489–495. http://dx.doi.org/10.1113/jphysiol.1981.sp013600

Nikolov, D.B., K. Xu, and J.P. Himanen. 2013. Eph/ephrin recognition and the role of Eph/ephrin clusters in signaling initiation. *Biochim. Biophys. Acta.* 1834:2160–2165. http://dx.doi.org/10.1016/j.bbapap.2013.04.020

Noberini, R., E. Rubio de la Torre, and E.B. Pasquale. 2012. Profiling Eph receptor expression in cells and tissues: A targeted mass spectrometry approach. *Cell Adhes. Migr.* 6:102–112. http://dx.doi.org/10.4161/cam.19620

Orioli, D., and R. Klein. 1997. The Eph receptor family: Axonal guidance by contact repulsion. *Trends Genet.* 13:354–359. http://dx.doi.org/10.1016/S0168-9525(97)01220-1

Park, S., and M.P. Sánchez. 1997. The Eek receptor, a member of the Eph family of tyrosine protein kinases, can be activated by three different Eph family ligands. *Oncogene.* 14:533–542. http://dx.doi.org/10.1038/sj.onc.1200857

Pette, D., and R.S. Staron. 1997. Mammalian skeletal muscle fiber type transitions. *Int. Rev. Cytol.* 170:143–223. http://dx.doi.org/10.1016/S0074-7696(08)61622-8

Pette, D., and R.S. Staron. 2001. Transitions of muscle fiber phenotypic profiles. *Histochem. Cell Biol.* 115:359–372.

Pette, D., and G. Vrbová. 1985. Neural control of phenotypic expression in mammalian muscle fibers. *Muscle Nerve.* 8:676–689. http://dx.doi.org/10.1002/mus.880080810

Rafuse, V.F., L.D. Milner, and L.T. Landmesser. 1996. Selective innervation of fast and slow muscle regions during early chick neuromuscular development. *J. Neurosci.* 16:6864–6877.

Reynolds, M.L., and C.J. Woolf. 1992. Terminal Schwann cells elaborate extensive processes following denervation of the motor endplate. *J. Neurocytol.* 21:50–66. http://dx.doi.org/10.1007/BF01206897

Sanes, J.R., and J.W. Lichtman. 1999. Development of the vertebrate neuromuscular junction. *Annu. Rev. Neurosci.* 22:389–442. http://dx.doi.org/10.1146/annurev.neuro.22.1.389

Sanes, J.R., L.M. Marshall, and U.J. McMahan. 1978. Reinnervation of muscle fiber basal lamina after removal of myofibers. Differentiation of regenerating axons at original synaptic sites. *J. Cell Biol.* 78:176–198. http://dx.doi.org/10.1083/jcb.78.1.176

Seiradake, E., A. Schaupp, D. del Toro Ruiz, R. Kaufmann, N. Mitakidis, K. Harlos, A.R. Aricescu, R. Klein, and E.Y. Jones. 2013. Structurally encoded intraclass differences in EphA clusters drive distinct cell responses. *Nat. Struct. Mol. Biol.* 20:958–964. http://dx.doi.org/10.1038/nsmb.2617

Smith, I.W., M. Mikesh, Y. Lee, and W.J. Thompson. 2013. Terminal Schwann cells participate in the competition underlying neuromuscular synapse elimination. *J. Neurosci.* 33:17724–17736. http://dx.doi.org/10.1523/JNEUROSCI.3339-13.2013

Soileau, L.C., L. Silberstein, H.M. Blau, and W.J. Thompson. 1987. Reinnervation of muscle fiber types in the newborn rat soleus. *J. Neurosci.* 7:4176–4194.

Son, Y.J., and W.J. Thompson. 1995a. Nerve sprouting in muscle is induced and guided by processes extended by Schwann cells. *Neuron.* 14:133–141. http://dx.doi.org/10.1016/0896-6273(95)90247-3

Son, Y.J., and W.J. Thompson. 1995b. Schwann cell processes guide regeneration of peripheral axons. *Neuron.* 14:125–132. http://dx.doi.org/10.1016/0896-6273(95)90246-5

Son, Y.J., J.T. Trachtenberg, and W.J. Thompson. 1996. Schwann cells induce and guide sprouting and reinnervation of neuromuscular junctions. *Trends Neurosci.* 19:280–285. http://dx.doi.org/10.1016/S0166-2236(96)10032-1

Stadler, H.S., K.M. Higgins, and M.R. Capecchi. 2001. Loss of Eph-receptor expression correlates with loss of cell adhesion and chondrogenic capacity in Hoxa13 mutant limbs. *Development.* 128:4177–4188.

Stark, D.A., R.M. Karvas, A.L. Siegel, and D.D.W. Cornelison. 2011. Eph/ephrin interactions modulate muscle satellite cell motility and patterning. *Development.* 138:5279–5289. http://dx.doi.org/10.1242/dev.068411

Swartz, M.E., J. Eberhart, E.B. Pasquale, and C.E. Krull. 2001. EphA4/ephrin-A5 interactions in muscle precursor cell migration in the avian forelimb. *Development.* 128:4669–4680.

Thompson, W.J., L.C. Soileau, R.J. Balice-Gordon, and L.A. Sutton. 1987. Selective innervation of types of fibres in developing rat muscle. *J. Exp. Biol.* 132:249–263.

Waddell, J.N., P. Zhang, Y. Wen, S.K. Gupta, A. Yevtodiyenko, J.V. Schmidt, C.A. Bidwell, A. Kumar, and S. Kuang. 2010. Dlk1 is necessary for proper skeletal muscle development and regeneration. *PLoS One.* 5:e15055. http://dx.doi.org/10.1371/journal.pone.0015055

Wang, H.U., and D.J. Anderson. 1997. Eph family transmembrane ligands can mediate repulsive guidance of trunk neural crest migration and motor axon outgrowth. *Neuron.* 18:383–396. http://dx.doi.org/10.1016/S0896-6273(00)81240-4

Whalen, R.G., D. Johnstone, P.S. Bryers, G.S. Butler-Browne, M.S. Ecob, and E. Jaros. 1984. A developmentally regulated disappearance of slow myosin in fast-type muscles of the mouse. *FEBS Lett.* 177:51–56. http://dx.doi.org/10.1016/0014-5793(84)80979-5

Wigmore, P.M., and D.J. Evans. 2002. Molecular and cellular mechanisms involved in the generation of fiber diversity during myogenesis. *Int. Rev. Cytol.* 216:175–232. http://dx.doi.org/10.1016/S0074-7696(02)16006-2

Wigston, D.J., and J.R. Sanes. 1982. Selective reinnervation of adult mammalian muscle by axons from different segmental levels. *Nature.* 299:464–467. http://dx.doi.org/10.1038/299464a0

Zuo, Y., J.L. Lubischer, H. Kang, L. Tian, M. Mikesh, A. Marks, V.L. Scofield, S. Maika, C. Newman, P. Krieg, and W.J. Thompson. 2004. Fluorescent proteins expressed in mouse transgenic lines mark subsets of glia, neurons, macrophages, and dendritic cells for vital examination. *J. Neurosci.* 24:10999–11009. http://dx.doi.org/10.1523/JNEUROSCI.3934-04.2004